# Automatic In-situ Optical Linearization of Silicon Photonic Ring-Assisted MZ Modulator for Integrated RF Photonic SoCs

**Md Jubayer Shawon,[1,*] and Vishal Saxena[1]**

[1] *Department of Electrical and Computer Engineering, University of Delaware, Newark, DE, 19716*

[*] *shawon@udel.edu*

**Abstract:** We experimentally demonstrate automatic optical linearization of a Ring-Assisted MZ modulator with SFDR $>$ 110dB.Hz$^{2/3}$, fabricated in a silicon photonic foundry process. The linearization algorithm reconfigures the modulator to its optimum SFDR or other desired regimes regardless of random phase offsets and process/temperature variations. 

## 1. Introduction

Electro-Optical (EO) modulators are one of the key elements of any RF photonic system. Traditionally, discrete lithium niobate ($LiNbO_3$) MZMs have widely been used in RF photonic systems. However, as the complexity of the system grows, there is a rapidly growing interest in the industry to realize EO modulators in a CMOS-compatible platform so that control electronics can be co-integrated. Silicon photonics has recently emerged as a disruptive technology platform where RF photonics components can be fabricated in the same process used for electronics. However, silicon-based EO modulators do not perform as well as their matured $LiNbO_3$ counterparts when it comes to linearity. Therefore, silicon-based EO modulator linearization is a topic of great interest. Recently, several research has been carried out where silicon-based MZM linearization has been attempted. These include electronic pre-distortion circuits [1] and third-order intermodulation (IM3) cancellation technique [2] in electronic domain. However, these are inherently narrowband approach and fails to take full advantage of the broadband nature of photonics. On the other hand, ring-assisted MZ Modulators (RAMZM) show great promise where the expansive voltage-to-phase response of the ring can be used to linearize compressive phase-to-amplitude response of MZM [3]. However, all previous implementations of RAMZM are hand-tuned [4] and require automatic tuning for wider adoption in large-scale RF photonic systems.

Therefore, in this work, we present a silicon-based reconfigurable RAMZM along with its automatic tuning algorithm. With this algorithm, the modulator can be automatically reconfigured to its optimum linear regime.

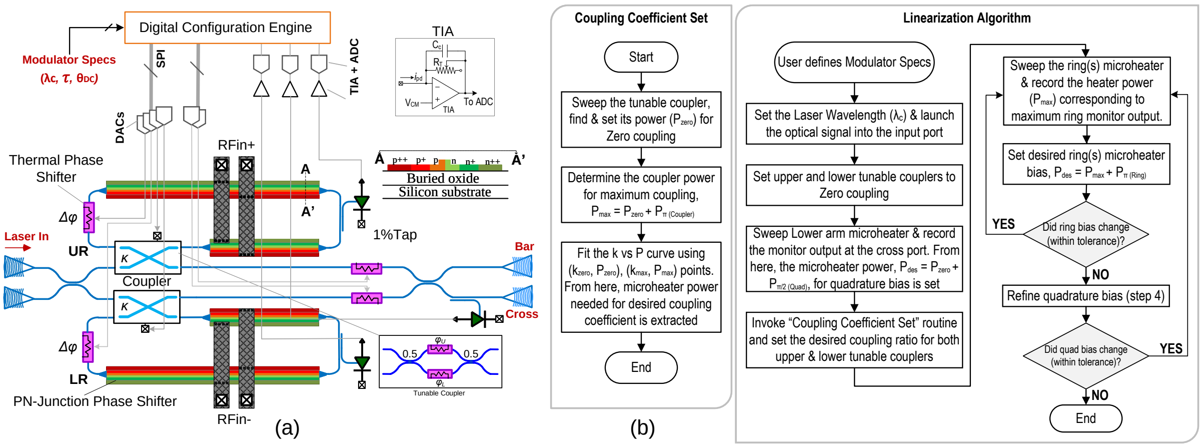


Fig. 1. (a) Schematic diagram of the RAMZM and its interfacing with the electronic backend. (b) Algorithm flowcharts for the automatic linearization of RAMZM leveraging the electronic backend.

## 2. Design, Fabrication and Packaging

As shown in Fig. 1(a), our RAMZM consists of a MZ structure with its arms coupled with ring modulators (UR/LR) via tunable couplers. Each of these rings has a high-speed phase modulator and microheater for resonance tuning. These phase modulators require differential inputs in order to operate at a linear regime. Each arm of the MZ structure is also loaded with microheaters to allow quadrature biasing. To enable automatic reconfiguration, we also implemented 1% monitor taps on each of the rings and 10% taps at the cross port of the modulator.

The RAMZM PIC has been fabricated in AIM Photonics foundry's 300mm wafer Active PIC process and occupies 1.38mm$^2$ area on the chip. Process-optimized grating couplers (GC) are used to get light in and out of the PIC. 220nm x 480nm silicon waveguides were utilized for interconnecting the optical components. Tunable couplers were implemented using a 2x2 thermo-optic switch, which is essentially a balanced MZ structure with microheaters on each arm. The microheater thermo-optic time constants are on the order of $\sim 15\mu$s. The 1% and 10% monitor taps used in this design are on-chip Ge photodetectors with couplers and optical terminations. To implement a high-speed phase modulator, we designed a 220nm x 450nm rib waveguide with $\sim$110nm etched silicon. As shown in the inset of Fig. 1(a), the silicon rib waveguide is lightly doped to form a lateral p-n junction at the center. Moderate doping was used in the region between the waveguide and the highly doped ohmic contact region. This region was 1$\mu$m away from the outer edges of the waveguide and provided a balanced tradeoff between the series resistance of the modulator and excess free carrier absorption.

The die is thinned to 150$\mu$m for better thermal control and wirebonded to a custom high-frequency PCB (RO4350B) in a COB assembly. As shown in Fig. 2, the COB assembly was co-packaged with a thermistor, Peltier cell, and thermo-electric cooler (TEC) controller in a closed loop to minimize the thermal crosstalk between tuning elements. The modulator RF feed comprises of impedance controlled single-ended/differential Coplanar Waveguides (CPWs) and end-launch connectors. The electronic backend used 16-channel 16-bit $\Delta\Sigma$ DACs, 3 tunable opamp-based transimpedance amplifiers (TIAs) and 16-channel multiplexed 16-bit $\Delta\Sigma$ ADCs. These data converters communicate with a microcontroller via SPI interface.

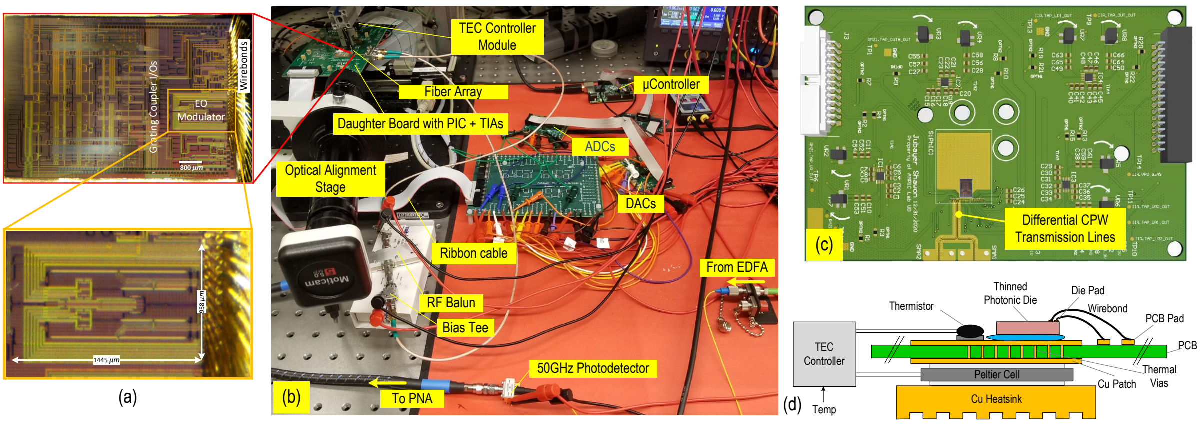


Fig. 2. (a) Micrograph of the RAMZM PIC in COB assembly. (b) Experimental setup with the RAMZM PIC aligned to a fiber array, interfaced with the electronic backend and measurement accessories (EDFA, PNA, PD). (c) The daughter board with the RAMZM PIC, transimpedance amplifiers and single-ended / differential CPW transmission lines. (d) COB assembly co-packaged with thermistor, Peltier cell and an external TEC controller board connected in a closed loop.

## 3. Linearization Algorithm, Experimental Setup and Results

As mentioned before, the linearization scheme relies upon the expansive voltage-to-phase response of the ring to compensate for the compressive raised cosine nonlinearity of the MZ. To achieve the best possible linearity, the RAMZM should be biased at $\{\phi_{bias}, \theta_{DC}\} = \{\frac{\pi}{2}, \pi\}$, where $\phi_{bias}$ and $\theta_{DC}$ are the quadrature bias of the MZ and ring bias, respectively [5]. Here, $\theta_{DC} = \pi$ signifies that the ring is at anti-resonance. On the other hand, the optimum transmission coefficient of the ring couplers is dependent upon loss factor within the ring and subject to link requirements [5]. Our algorithm (shown in Fig. 1b) is capable of dialing any coupling coefficients as per the user-provided specs. In order to linearize the modulator, our algorithm requires some pre-characterizations of the tuning elements. The pre-characterization process includes recording microheater Voltage vs Power characteristics, $P_\pi$ of the tunable coupler microheaters, $P_\pi$ of the ring microheaters and $P_{\pi/2}$ of the lower arm microheaters. Here, $P_\pi$ and $P_{\pi/2}$ signifies power required for $\pi$ and $\pi/2$ phase shifts, respectively. These were extracted using SMU, tunable laser and photodetectors. It is important to note that, these pre-characterizations are only performed once. Once these data are stored, no future pre-characterizations is required. Also, these characterizations can be performed fully automatic and in-situ.

The experimental setup consists of the electronic backend for tuning, a Keysight N5225B PNA, EDFA, and a 50GHz photodetector (PD) with high linearity. A single-ended RF input is applied to an RF balun which converts it to a differential signal pair. These differential signals pass through a bias-tee which provides DC offset to the modulation signal. In this work, we biased the phase modulators at -3.5V. The differential signals are then applied to one of each ring and the DUT output is recorded using a linear PD (after passing through an EDFA). Fig. 3(a)-(f) shows modulator spectral response at different stages of tuning. The reconfiguration process took ∼370s. After the reconfiguration was complete, power sweep of two RF tones centered around 1.1GHz and 10MHz apart are applied to the DUT and the SFDR value is calculated from the relative power of the intermodulation tones. As can be seen from Fig. 3(g)-(h), the reconfigured RAMZM shows significantly higher linearity compared to when it is not configured.

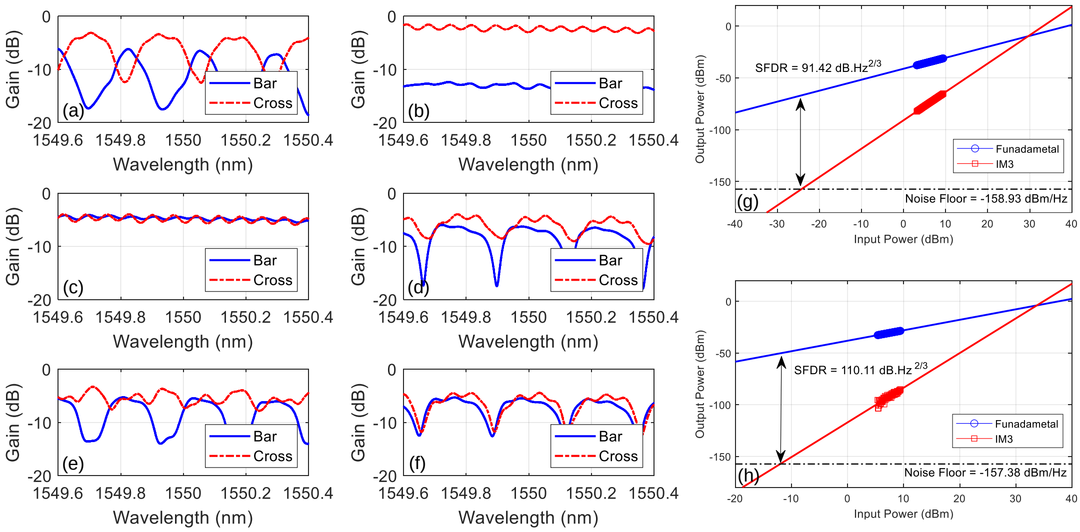


Fig. 3. Experimentally measured bar and cross port responses of RAMZM PIC when (a) No bias is applied, (b) Upper and lower couplers are set to zero coupling, (c) Quadrature bias is set, (d) Upper and lower couplers are set to the desired coupling coefficient (e) Upper ring anti-resonance is aligned to 1550nm, (f) Anti-resonance of both rings is aligned to 1550nm; Experimentally measured SFDR of RAMZM PIC with (g) No linearization, (h) Optical domain linearization.

## 4. Conclusion

We demonstrated a RAMZM PIC that can be reconfigured at different biasing regimes based on the user specs. Leveraging our tuning algorithm, we experimentally demonstrated the optical domain linearization of RAMZM with SFDR $>$ 110dB.Hz$^{2/3}$ at 1.1GHz. Moreover, the presented RAMZM PIC is fabricated in a CMOS-compatible SiP foundry process. By taking full advantage of the low-cost CMOS fabrication process, this reconfigurable EO modulator can be widely used as a plug-n-play module in integrated RF Photonic SoCs.

## References


1. J. Okyere, K. Yu, K. Entesari, and S. Palermo, “A fifth-order polynomial predistortion circuit for mach-zehnder modulator linearization in 65nm cmos,” in *2017 Texas Symposium on Wireless and Microwave Circuits and Systems (WMCS),* (IEEE, 2017), pp. 1–4.
2. N. Hosseinzadeh, A. Jain, R. Helkey, and J. F. Buckwalter, “A distributed low-noise amplifier for broadband linearization of a silicon photonic mach–zehnder modulator,” IEEE J. Solid-State Circuits **56**, 1897–1909 (2020).
3. J. Cardenas, P. A. Morton, J. B. Khurgin, A. Griffith, C. B. Poitras, K. Preston, and M. Lipson, “Linearized silicon modulator based on a ring assisted mach zehnder inteferometer,” Opt. express **21**, 22549–22557 (2013).
4. C. Zhang, P. A. Morton, J. B. Khurgin, J. D. Peters, and J. E. Bowers, “Ultralinear heterogeneously integrated ring-assisted mach–zehnder interferometer modulator on silicon,” Optica **3**, 1483–1488 (2016).
5. J. Yang, F. Wang, X. Jiang, H. Qu, M. Wang, and Y. Wang, “Influence of loss on linearity of microring-assisted mach-zehnder modulator,” Opt. Express **12**, 4178–4188 (2004).